

# Synthesis and functionalization of superparamagnetic poly- $\epsilon$ -caprolactone microparticles for the selective isolation of subpopulations of human adipose-derived stem cells

Elizabeth R. Balmayor<sup>1,2,\*</sup>, Iva Pashkuleva<sup>1,2</sup>, Ana M. Frias<sup>1,2</sup>,  
Helena S. Azevedo<sup>1,2,\*</sup> and Rui L. Reis<sup>1,2</sup>

<sup>1</sup>*3B's Research Group – Biomaterials, Biodegradables and Biomimetics, University of Minho, Headquarters of the European Institute of Excellence on Tissue Engineering and Regenerative Medicine, AvePark, 4806-909 Taipas, Guimarães, Portugal*

<sup>2</sup>*IBB – Institute for Biotechnology and Bioengineering, PT Government Associated Laboratory, Guimarães, Portugal*

There has been a growing interest in using biofunctionalized magnetic particles for cell isolation. This paper describes the synthesis and characterization of magnetite-polymer (Fe<sub>3</sub>O<sub>4</sub>-poly- $\epsilon$ -caprolactone, magnetite-PCL) microparticles surface functionalized with amino and epoxy groups allowing easy covalent attachment of specific antibodies and subsequent ability to bind target cells. Particles with different sizes (4–135  $\mu$ m), spherical shape and superparamagnetic behaviour (magnetite content of about 13 wt%) were obtained. The functionalized microparticles presented high protein-binding capacity (coupling efficiency of 47% for epoxy- and 71% for amino-functionalized particles) with a low level of non-specific binding. We have further investigated the influence of initial protein concentration, pH, ionic strength, temperature and incubation time on the capacity of amino-functionalized particles to bind protein molecules. The results showed that maximum protein coupling is rapidly achieved ( $\leq 5$  h) at pH 5.5 and low ionic strength (0.05 M NaCl). Furthermore, when cultured in direct contact with osteoblast-like cells (Saos-2) or human-derived adipose stem cells (ASCs), the amino-functionalized particles did not affect the proliferation and morphology of the cells. As a proof of principle for the application of magnetic microparticles for cell isolation, CD105 (endoglin) antibody was coupled to the magnetic particle surface to bind subpopulations of human ASCs expressing the CD105 antigen. The isolation of CD105+ ASCs from a heterogeneous cell population was confirmed by flow cytometry analysis. Given the demonstrated potential of functionalized magnetite-PCL microparticles for selective cell isolation, we expect that these particles may be further applied in immuno-magnetic cell separation owing to their versatility and ease of surface modification.

**Keywords:** particulate materials; magnetic properties; surface chemistry; cell recognition

## 1. INTRODUCTION

The interest and use of cell sorting for applications in cell research therapy continue to increase. Cell separation by applying an external magnetic field is among some of the most efficient methods for bulk cell separation. In this method, cells bind to cell-affinity ligands on the surface of magnetic particles and are then

separated from the bulk of the sample using magnetic forces (figure 1).

Superparamagnetic particles, with no residual magnetism upon magnetic field removal, are available with carboxyl or amino groups on their surface allowing the easy attachment of target ligands (e.g. antibodies). Many companies offer particles with the desired size and surface functionality for applications in cell isolation [1–3], protein separation [4–6] and diagnostics [3,7–9]. Although much is now commercially available, the development of new types of magnetic particles and their surface modification are still an area of ongoing research. Superparamagnetism, uniform and adequate

\*Authors for correspondence (erosado@dep.uminho.pt, hazevedo@dep.uminho.pt).

Electronic supplementary material is available at <http://dx.doi.org/10.1098/rsif.2010.0531> or via <http://rsif.royalsocietypublishing.org>.

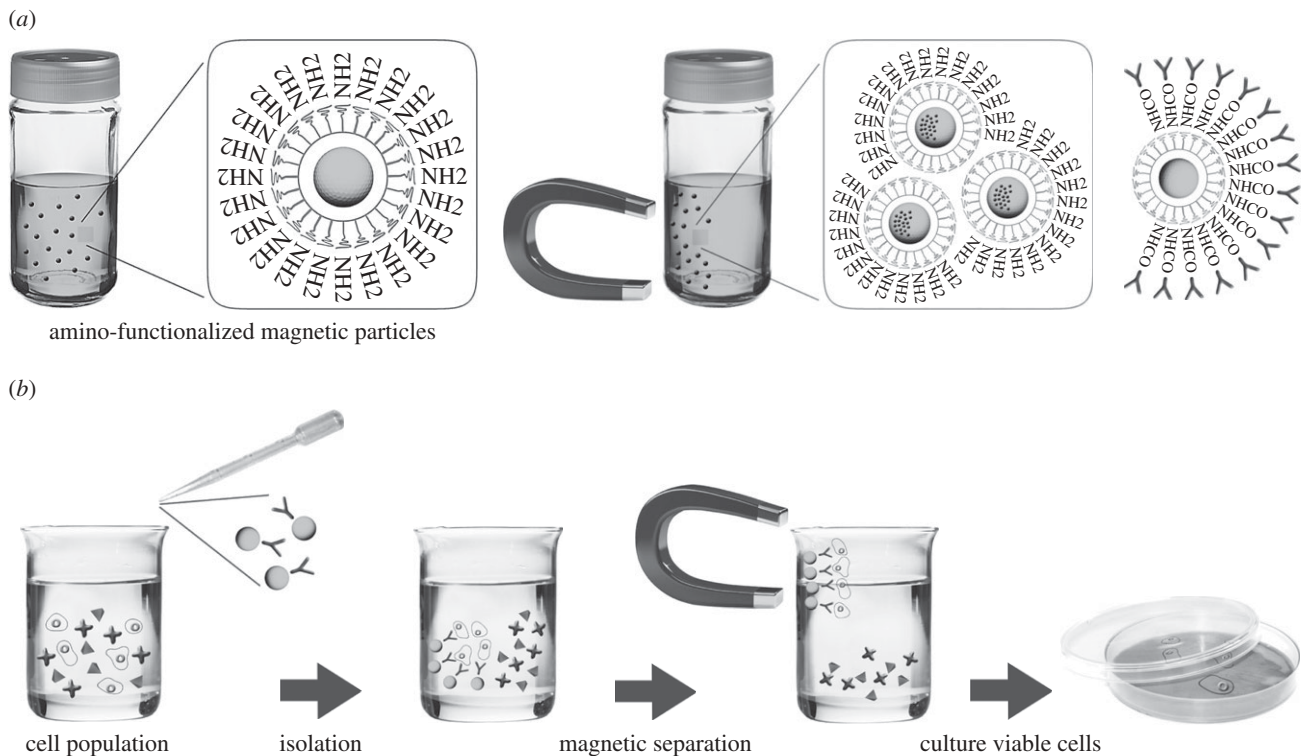


Figure 1. Schematic representation of (a) surface-functionalized magnetic particles and (b) the principle of cell isolation using these particles.

size distribution, and functionalized surface are considered the most important characteristics in the design and formulation of microparticles for cell isolation.

Usually, magnetite nanoparticles consist of an aqueous dispersion of iron (II, III) oxide ( $\text{Fe}_3\text{O}_4$ ) particles with average size in the nanoscale (50–200 nm) and presenting superparamagnetic properties [10]. The magnetite nanoparticles can be covered with organic or inorganic compounds to protect them against aggregation by foreign ions and promote their stability. Polymeric materials have been widely used for this purpose [1,11–15] because they have several advantages as coating materials. They are in general non-toxic, presenting great processing versatility and ability for surface functionalization. The most commonly used polymers have been polystyrene, divinylbenzene and poly(methylmethacrylate) [13,16–18]. The preparation of polystyrene microparticles involves laborious polymerization reactions and they use highly toxic compounds. In this work, we have chosen poly- $\epsilon$ -caprolactone (PCL) as the polymeric matrix to contain the magnetite nanoparticles, knowing its demonstrated biocompatibility [19–22], processing versatility [23] and ease of surface modification [24,25]. Furthermore, PCL has been approved by the Food and Drug Administration (FDA) as a bioabsorbable suture and drug-delivery biomaterial, making it an attractive material for isolation of human cells.

Particle binding to cells can occur either specifically, by attaching to specific receptors on the cell surface, or non-specifically, by general interaction with one or more components of the cell membrane [26]. In both cases, binding is expected to be governed by the nature of the particle, including its size, composition and surface properties. Functionalization of the surface with amino,

epoxy and carboxyl groups allows the covalent attachment of target ligands such as proteins [1,6]. Contrary to passive adsorption, covalent immobilization provides a stable material–biomolecule conjugate and avoids non-specific binding [27,28].

To the best of our knowledge, the development of superparamagnetic-PCL (m-PCL) microparticles with suitable features for isolation of cells has not been reported before. We believe that considerable efforts will be directed to this area of research as functionalization of microparticle surfaces with target ligands will increasingly be used to control the interaction of microparticles with cells.

## 2. RESULTS AND DISCUSSION

Immunomagnetic separation of cells using superparamagnetic particles or beads coated with antibodies against surface antigens has been extensively investigated [1–3,29]. It is a very selective and mild technology because it permits rapid and efficient isolation of target cell populations. The cells bound to the magnetic particles remain viable and thereafter they can be expanded by placing the isolated fraction in suitable culture media.

Particle binding to cells is expected to be governed by its size and surface properties. We have, therefore, investigated these parameters in detail during the preparation of m-PCL microparticles.

### 2.1. Preparation of superparamagnetic PCL microparticles

Magnetite ( $\text{Fe}_3\text{O}_4$ ) nanoparticles were obtained by adapting a classical co-precipitation method patented

Table 1. The effect of experimental conditions used for the production of m-PCL microparticles on their size, magnetite content and magnetic properties.

sample	magnetite/ polymer ratio	PVA (%)	stirring rate (r.p.m.)	particle size ( $\mu\text{m}$ ) $\pm$ s.d.	magnetite content (%) <sup>a</sup>	$M_s/300\text{ K}$ ( $\text{emu g}^{-1}$ )	$m_r/300\text{ K}$
m-PCL 1	0.005	1	11 000	$93.7 \pm 8.3$	0.59	3.8	0.2849
m-PCL 2	0.05	1	11 000	$97.4 \pm 10.3$	4.19	4.2	0.2530
m-PCL 3	0.10	1	11 000	$107.0 \pm 9.2$	10.34	4	0.3103
m-PCL 4	0.15	1	11 000	$134.1 \pm 7.5$	13.13	4.6	0.3007
m-PCL 5	0.10	0.5	11 000	$112.0 \pm 4.8$	n.a.	n.a.	n.a.
m-PCL 6	0.10	1	11 000	$97.2 \pm 11.0$	n.a.	n.a.	n.a.
m-PCL 7	0.10	2	11 000	$82.6 \pm 8.3$	n.a.	n.a.	n.a.
m-PCL 8	0.10	1	11 000	$104.0 \pm 5.2$	n.a.	n.a.	n.a.
m-PCL 9	0.10	1	20 000	$52.1 \pm 6.9$	n.a.	n.a.	n.a.
m-PCL 10	0.10	1	24 000	$4.2 \pm 2.1$	n.a.	n.a.	n.a.

<sup>a</sup>Determined by thermogravimetric analysis.

by Khalafalla & Reimers [30]. Oleic acid was added during the synthesis to provide hydrophobicity and adequate stability for the nanoparticle suspension. Figure 2a presents a transmission electron microscopy image of magnetite nanoparticles. They exhibit a regular spherical shape with the absence of nanoparticle aggregates. The collected selected area electron diffraction data (figure 2b) confirm the presence of well-defined broad diffraction rings typically observed in  $\text{Fe}_3\text{O}_4$  structures (311) and (220). Dynamic light scattering measurements (figure 2c) show a mean diameter of 50 nm and narrow size distribution.

The magnetite nanoparticles were further entrapped within a PCL matrix to form the m-PCL microparticles. Particles with spherical shape, smooth surface and different sizes (4–135  $\mu\text{m}$ ) were obtained (figure 2d and table 1). Particle size is an important parameter in cell isolation, as it dictates the specific interaction with cells [2,10,31]. Studies have reported cellular internalization of various sized particles from several nanometres to 3  $\mu\text{m}$  [26]. In most current cell-isolation techniques, the magnetic particles bind to the cell surface and particle internalization by cells is not essential. Particles of larger size may, however, not be efficient owing to the lack of interaction with cells (with a typical size of 10–100  $\mu\text{m}$ ). The type of cell also adds a level of complexity, as particle binding can vary depending on cell type and cell surface properties. Magnetic particles used for batch cell separation typically have diameters of 50 nm (Miltenyi Biotec), 200 nm (Estapor), 1.5  $\mu\text{m}$  (BioMagic, Biopal) to 2.8  $\mu\text{m}$  and 4.5  $\mu\text{m}$  Dynabeads (Invitrogen) [32].

We found that the size of m-PCL microparticles could be controlled by varying several parameters used during their preparation such as magnetite to polymer ratio, polyvinyl alcohol (PVA) concentration and stirring rate (table 1).

The magnetite to polymer ratio was varied in the range 0.005–0.15. The increase in the magnetite content resulted in the formation of larger size polydisperse particles, but it did not influence the surface morphology and spherical shape of the particles. PVA was used as emulsifier and stabilizing agent during the particle formation. It has been previously reported that concentrations of PVA higher than 2 per cent can induce

changes in the particle morphology, which can result in the loss of spherical shape [33]. Therefore, the effect of PVA concentration was also studied by varying its content in the emulsification medium, from 0.5 up to 2 per cent. The size of the microparticles slightly decreases as the PVA concentration increases (table 1), while the shape and surface morphology of the particles are not affected. Hence, we can state that PVA concentration up to 2 per cent is suitable for the preparation of particles using the emulsification method. The stirring rate is the parameter with the most pronounced influence on the size of the m-PCL microparticles. A monodisperse m-PCL microparticle population, with a size of  $4.2 \pm 2.1\ \mu\text{m}$ , was obtained when a stirring rate of 24 000 r.p.m. was used (table 1 and figure 2d). Size distribution analysis for a representative sample, m-PCL 7, showed that the microparticles exhibited unimodal distributions centred on a population with sizes between 60 and 100  $\mu\text{m}$  (figure 2f). However, subpopulations with different sizes are also obtained within a narrow size range. The individual collection of these subpopulations can result in the possibility of using a set of particles, produced under the same experimental conditions, but with different sizes and narrow size range.

## 2.2. Characterization of m-PCL microparticles

The Fourier-transformed infrared (FTIR) spectrum of m-PCL microparticles confirmed the presence of the magnetite entrapped within the PCL matrix. The characteristic broad band at  $580\ \text{cm}^{-1}$  was observed in the spectra of both synthesized magnetite and m-PCL microparticles (figure 3b). Characteristic bands of PCL around 1750, 1238 and  $1172\ \text{cm}^{-1}$ , which correspond to C=O, asymmetric COC, OC–C and symmetric COC stretchings, respectively, are present in PCL microparticles with and without entrapped magnetite.

X-ray diffraction (XRD) was used to confirm the crystalline structure of the obtained magnetite nanoparticles (figure 3c). The XRD pattern confirmed the magnetite ( $\text{Fe}_3\text{O}_4$ ) structure for the nanoparticles with detected peaks at 29.94, 35.4, 43.01, 53.4 and 56.96  $2\theta$  degree (consistent with the standard data for magnetite JCPDS card 19-0629). The XRD pattern of

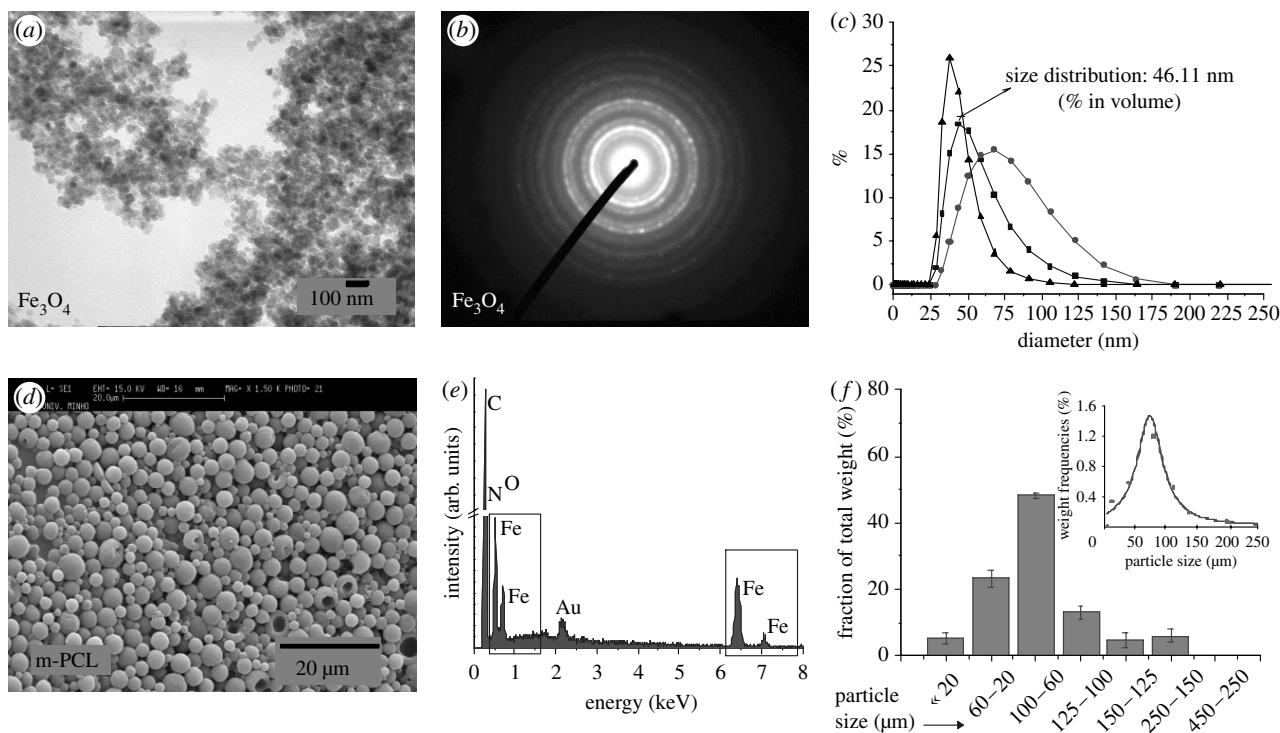


Figure 2. (a) Transmission electron microscopy image and (b) selected area electron diffraction pattern of synthesized magnetite nanoparticles. (c) Size distribution of magnetite nanoparticles in water–glycerine (1 : 1, v : v) suspension measured by dynamic light scattering (filled squares, volume; filled circles, intensity; filled triangles, number). (d) Scanning electron micrograph (SEM) and (e) energy-dispersive (EDS) spectrum of magnetic poly- $\epsilon$ -caprolactone (m-PCL 10; table 1) microparticles (note: the presence of the Au peak is associated with the coating of the samples for SEM–EDS analysis). (f) Size distribution of the m-PCL microparticles (m-PCL 7, table 1) quantified by sieve analysis. Inset graph in (f) represents the distribution of particle size by weight.

m-PCL microparticles shows identical peaks, demonstrating the entrapment of the magnetite in the PCL matrix. The broadening of the peaks observed in the pattern of the m-PCL microparticles is consistent with the composite nature of the microparticles.

The amount of magnetite present in the m-PCL microparticles was investigated by thermogravimetric analysis (TGA). TGA was performed under  $N_2$  atmosphere to minimize the mass increase owing to iron oxidation, but allowing the polymer to thermally decompose. TGA thermograms (electronic supplementary material, figure S1) obtained for the m-PCL microparticles show a continuous weight loss in the range of 300–400°C, which corresponds to the decomposition of PCL [34]. The remaining mass after this temperature corresponds to the iron content of the sample. The amount of entrapped magnetite coincides with the initial amount of magnetite added in the solution for the m-PCL preparation (table 1).

The magnetic properties of m-PCL microparticles are of key importance for their subsequent application in selective cell isolation. We have, therefore, measured the saturation magnetization ( $M_s$ ), relative saturation remnance ( $m_r = M_r/M_s$ ) and coercivity of remnance ( $H_c$ ) of the synthesized magnetite nanoparticles and m-PCL microparticles and the results are presented in table 1 and figure 4.

The measurements were performed at room (300 K) and low temperature (5 K), at which magnetite presents a characteristic magnetic behaviour. The magnetite

nanoparticles exhibited superparamagnetic behaviour at room temperature with saturation magnetization  $M_s = 15.7 \text{ emu g}^{-1}$  (figure 4a). This value of  $M_s$  is lower than the one reported for magnetite [35]. This phenomenon has been observed and explained earlier by other authors [11] and can be related to the use of oleic acid (40% relative to the amount of produced magnetite) to coat the nanoparticles during their preparation. Lower values were also obtained for  $m_r$  (0.0637) indicating a typical superparamagnetic behaviour, i.e. the absence of magnetic memory of the sample once the applied field is removed. When the temperature was decreased to 5 K, the saturation of magnetization increased to values of  $51.5 \text{ emu g}^{-1}$  and the presence of broader hysteresis loop was observed (figure 4a:  $H_c = 250 \text{ Oe}$ ,  $m_r = 0.2544$ ). The increment of the magnetization at low temperature can be related to the correspondent decline of the magnetocrystalline anisotropy. The fact that an incomplete saturation of the magnetization was observed at 5 K can be related to the presence of small grains (owing to the nature of the sample), which also explains the gradual increment in  $M_s$  value after saturation. Moreover, at lower temperature there is a rearrangement of the  $Fe^{2+}$  and  $Fe^{3+}$  ions in the unit cell (magnetite crystallizes with spinel structure) with the consequent variation of the configuration of the magnetic moments in the unit cell [36,37]. Figure 4b presents the magnetization curves of the m-PCL microparticles. A typical superparamagnetic behaviour without any hysteresis loop

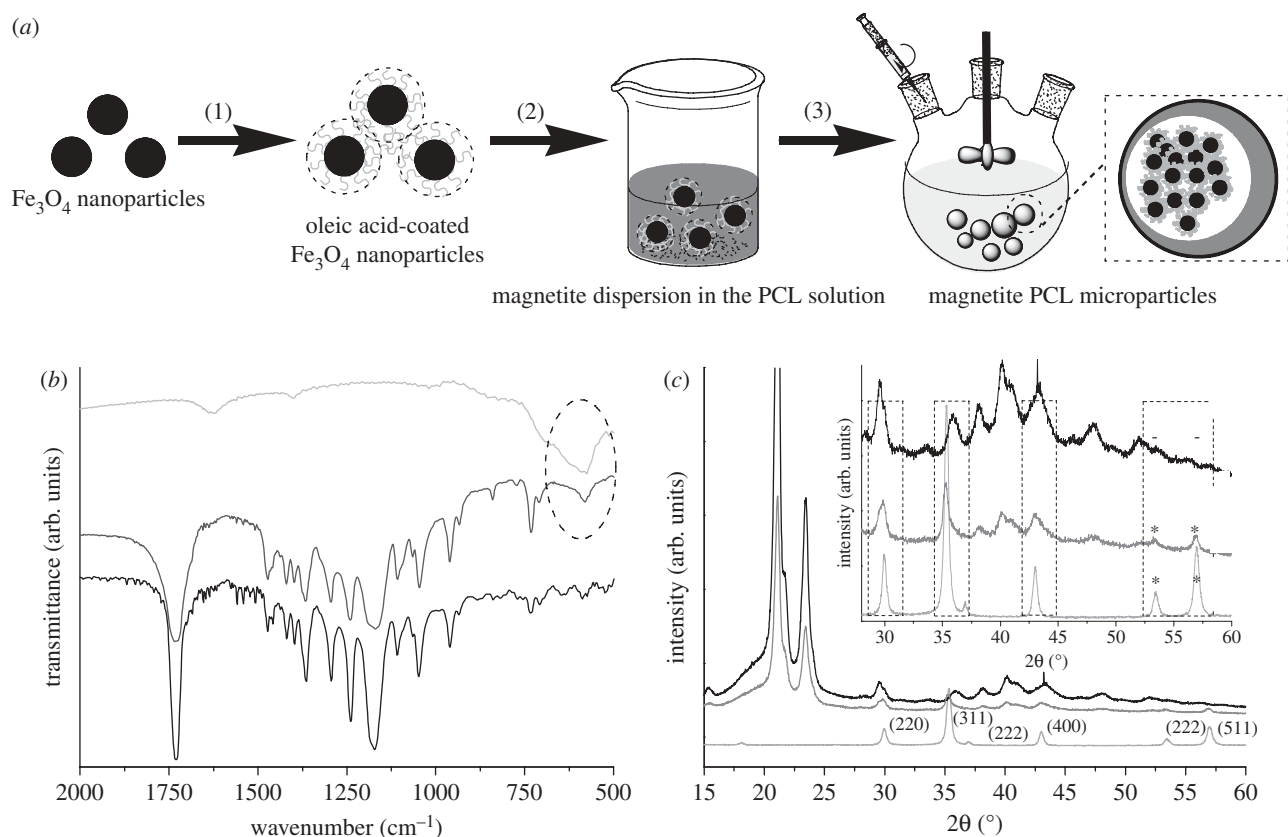


Figure 3. (a) Schematic representation of the set-up for the preparation of m-PCL microparticles. (b) FTIR spectra and (c) XRD patterns of m-PCL microparticles. The characteristic band of magnetite in FTIR spectra is marked with an oval. Inset graph in (c) is a zoom-in showing the XRD pattern with identified characteristic peaks of magnetite in the m-PCL microparticles (\*) (JCPDS card 19-0629). Magnetite nanoparticles and magnetite-free PCL microparticles were used as control samples in both FTIR and XRD analysis. Light grey, Fe<sub>3</sub>O<sub>4</sub>; dark grey, PCL microparticles; black, m-PCL microparticles.

and with low values of magnetic remnance ( $m_r = 0.0637$ ) was observed. The entrapment of the magnetite nanoparticles into the PCL matrix resulted in a decrease in the saturation magnetization value to  $4 \text{ emu g}^{-1}$ . The decrease in magnetization is due to the fact that the polymer (PCL) has no magnetic properties. An excellent isolation of the m-PCL microparticles from the suspension can however be observed when a magnet is placed near the container (figure 4c). Superparamagnetism was also observed upon removal of the external magnetic field.

After studying the effect of different parameters on the particle properties, we have selected particles of about  $50 \mu\text{m}$  to conduct the subsequent studies (surface functionalization, protein coupling, cell viability and proliferation, and cell isolation).

### 2.3. Surface functionalization of m-PCL microparticles

Amino-functionalized m-PCL microparticles were obtained by an aminolysis reaction. The presence of  $-\text{NH}_2$  groups on the modified m-PCL microparticles ( $\text{NH}_2\text{-m-PCL}$ ) was quantified by the ninhydrin colorimetric method. The absorbance, determined after functionalization, is significantly higher in comparison with the untreated microparticles, clearly confirming the presence of amino groups on the surface. By controlling

the 1,6-hexanediamine concentration, reaction temperature and time, surfaces with different amino group densities were obtained (table 2). The amount of  $-\text{NH}_2$  groups on the m-PCL microparticle surface increases with the aminolysis time and 1,6-hexanediamine concentration. However, for aminolysis time longer than 60 min and 1,6-hexanediamine concentration higher than 10 per cent, the density of the  $-\text{NH}_2$  groups decreases slightly. It was found that the temperature used during the aminolysis reaction does not influence the density of amino groups. The highest density ( $5.0 \pm 0.2 \times 10^{-7} \text{ mol mg}^{-1}$ ) was obtained for a reaction time of 60 min with 10 per cent of 1,6-hexanediamine.

The functionalized microparticles were analysed by X-ray photoelectron spectroscopy (XPS). The results from XPS are summarized in table 3. We have observed the presence of Fe in the survey spectra for all the studied materials, evidence of the magnetite present on the surface of the m-PCL microparticles. The detection of Si is due to the silicon wafers used as support for the sample preparation. Nitrogen was detected only for the  $-\text{NH}_2$ -functionalized m-PCL microparticles, confirming the success of the functionalization. XPS analysis did not show any significant difference between epoxy-modified and unmodified m-PCL microparticles. Previous studies have also reported some difficulties in the characterization of epoxy groups on the surface of particles and films by XPS [38,39]. To confirm

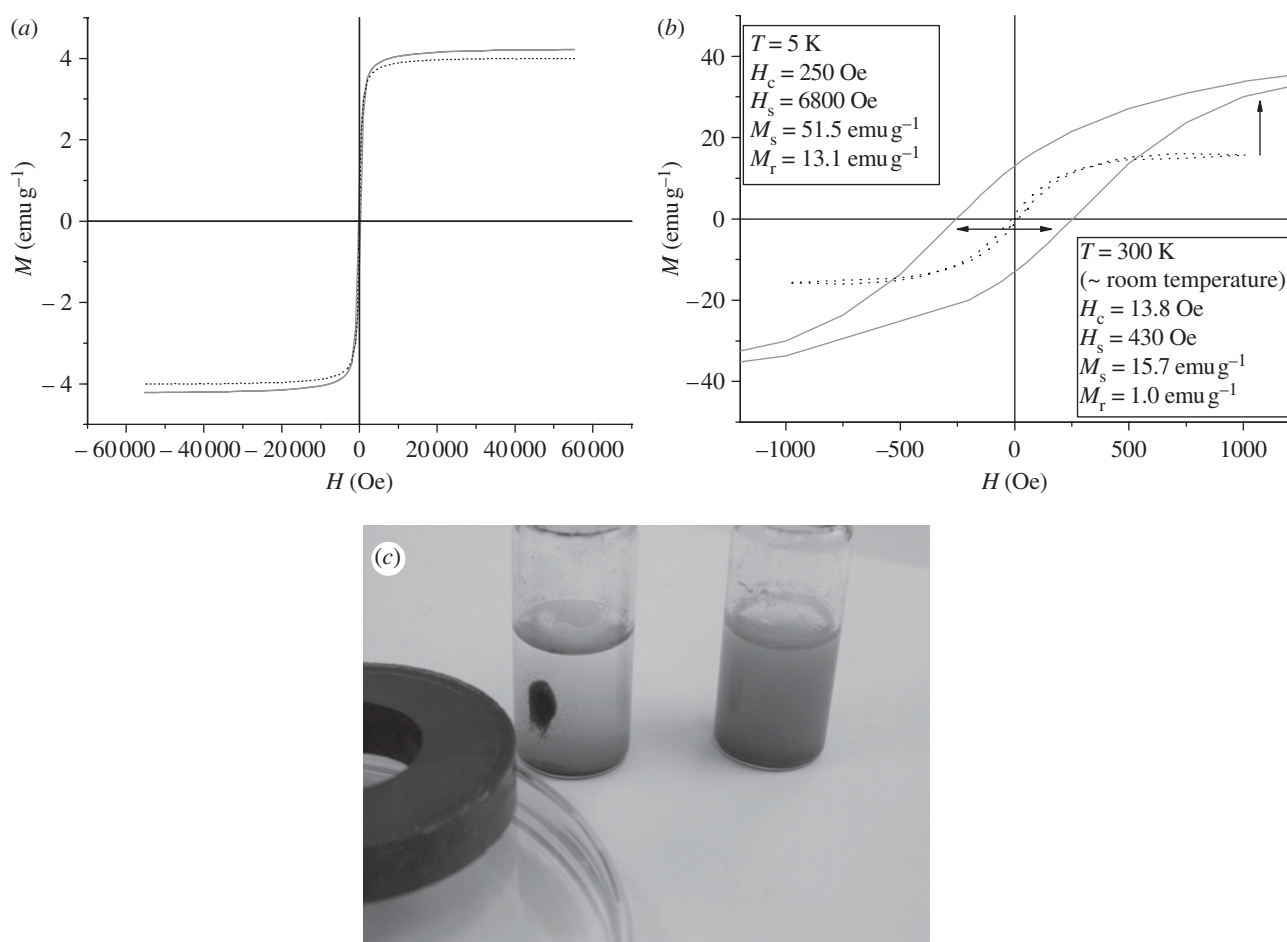


Figure 4. (a) Hysteresis loops of synthesized magnetite nanoparticles and (b) m-PCL microparticles. Solid line,  $T = 5$  K; dotted line,  $T = 300$  K. (c) Photograph shows the stability of the m-PCL microparticles dispersed in water (right vial) and their response to an external magnetic field (left vial).

Table 2. NH<sub>2</sub> density (ninhydrin assay) as a function of the conditions employed for surface functionalization of m-PCL microparticles.

sample	aminolysis time (min)	1,6-hexanediamine (%)	aminolysis temperature (°C)	NH <sub>2</sub> density ( $\times 10^{-7}$ mol mg <sup>-1</sup> )
m-PCL	—	—	—	$0.007 \pm 0.19$
NH <sub>2</sub> -m-PCL 1	30	10	37	$5.59 \pm 0.43$
NH <sub>2</sub> -m-PCL 2 <sup>a</sup>	60	10	37	$6.27 \pm 0.33$
NH <sub>2</sub> -m-PCL 3	90	10	37	$5.54 \pm 0.56$
NH <sub>2</sub> -m-PCL 4	60	2	37	$3.69 \pm 0.40$
NH <sub>2</sub> -m-PCL 5	60	5	37	$4.06 \pm 0.27$
NH <sub>2</sub> -m-PCL 6	60	20	37	$4.08 \pm 0.59$
NH <sub>2</sub> -m-PCL 7	60	10	25	$5.84 \pm 0.83$

<sup>a</sup>NH<sub>2</sub>-m-PCL microparticles with the highest amount of NH<sub>2</sub> surface groups, thus selected for protein-binding experiments.

the surface functionalization, we performed additional experiments, namely protein-binding studies and confocal laser scanning microscopy (CLSM).

#### 2.4. Protein coupling on functionalized m-PCL microparticles

We next investigated the possibility to covalently attach protein molecules to our microparticles. Towards this objective, we have performed protein-coupling experiments using bovine serum albumin (BSA) as a

model protein. To achieve protein covalent binding to the amino-functionalized m-PCL microparticles, a carbodiimide coupling was followed, while direct protein attachment was performed for epoxide-functionalized particles. Different conditions, in terms of initial protein concentration, pH, ionic strength and incubation time, were studied in the protein-binding experiments (figure 5).

Analysis of the results presented in figure 5a indicates that, as expected, a higher amount of protein is bound to the surface of functionalized m-PCL

Table 3. Surface chemical composition of functionalized m-PCL microparticles determined by XPS.

sample	%C	%O	%Fe	%N	%Si	%Na
m-PCL	57.4	28.4	0.7	n.f.	12.9	0.7
plasma-treated m-PCL	69.1	28.2	0.5	n.f.	1.4	0.7
epoxy-functionalized m-PCL	57.8	29.0	0.5	n.f.	10.7	2.1
amino-functionalized m-PCL	57.3	27.4	0.7	0.8	13	0.8

microparticles in comparison with untreated and plasma-treated controls. The highest amount of bound protein was found when NH<sub>2</sub>-m-PCL microparticles (*N*-(3-dimethylaminopropyl)-*N'*-ethylcarbodiimide hydrochloride (EDC)-mediated reaction) were used. For both surface-activated microparticles, protein-coupling experiments were carried out at pH 5.5. At this pH, EDC reaction is highly favoured, whereas epoxide chemistry is favoured at neutral to alkaline pH. Consequently, the amount of bound protein to NH<sub>2</sub>-m-PCL microparticles via EDC is higher.

Proteins will initially occupy the microparticle surface. On increasing the amount of added protein, a binding plateau is reached. Saturation of the surface functional groups by protein molecules is most probably the explanation for this result. Above a certain value of initial protein concentration, there are no more available groups for covalent coupling of additional protein molecules. Consequently, the amount of bound protein remains constant.

NH<sub>2</sub>-m-PCL microparticles were selected for further study of the effect of experimental conditions on protein coupling.

Figure 5*b* shows the influence of pH on protein binding on NH<sub>2</sub>-m-PCL microparticles. The maximum protein binding was obtained at pH 5.5. The activation of the carboxyl groups of proteins by EDC is favoured at acidic pH. At lower pH, the amino groups at the microparticle surface are highly protonated (NH<sub>3</sub><sup>+</sup>) and therefore not involved in the coupling reaction. Furthermore, at this pH (below BSA isoelectric point), the net charge of protein is positive, resulting in electrostatic repulsion [40,41]. The overall result is a decrease in protein binding at pH 3.5.

At pH 7, lower protein coupling was also observed. Although it is reported that the EDC-mediated reaction can still take place at pH 7 [42], this reaction is not favoured at neutral to basic pHs.

The effect of ionic strength on protein binding was studied by increasing the salt (NaCl) concentration. Figure 5*c* shows the protein-binding isotherms on NH<sub>2</sub>-m-PCL microparticles in 2-(*N*-morpholino)ethanesulphonic acid (MES) buffer at pH 5.5 and ionic strength in the range of 0.05–1.5 M. A drastic decrease in the bound protein was obtained at higher salt concentrations. The interaction of free carboxylic groups of proteins with ionic species might hinder their availability to participate in the formation of amide bonds, thus leading to lower binding yields [43].

Increasing the incubation time from 5 h to overnight did not show any significant influence on the amount of

bound protein (figure 5*d*). Five hours of incubation seems to be enough to allow reaction between the amino groups present at the microparticles surface with free carboxylic groups on the protein molecules. Similarly, no difference was observed on the amount of bound protein when the temperature changed from 25°C to 37°C.

Protein adsorption can occur at the material surface through hydrophobic and/or electrostatic interactions [44,45]. Weakly bound protein can be eluted by repeated washings with buffer solutions containing surfactants. We have used Tween 20 surfactant to remove adsorbed protein and the remaining protein in the supernatant was quantified to determine the amount covalently coupled. Table 4 summarizes the values obtained for covalently bound protein to both amino- and epoxy-functionalized surface. About 70 per cent of protein was covalently bound on the amino-activated and 47 per cent on the epoxy-activated surface.

CLSM was used to visualize the covalently coupled protein (figure 5*e,f*). Fluorescein isothiocyanate (FITC)-labelled BSA was employed during the binding experiments. CLSM results confirmed the successful surface functionalization proposed in this work (amino and epoxy) and consequently the covalent binding of the FITC-BSA on the microparticles surface. The observed fluorescence was more intense when NH<sub>2</sub>-m-PCL microparticles were used (figure 5*e*), which confirms a higher coupling efficiency for these microparticles in comparison with the epoxy-functionalized ones (figure 5*f*).

### 2.5. Cell viability and proliferation in contact with m-PCL microparticles

The effect of m-PCL microparticles on cell viability and proliferation was followed-up to 7 days by 3-(4,5-dimethylthiazol-2-yl)-5-(3-carboxymethyl-2-oxophenyl)-2-(4-sulphophenyl)-2H-tetrazolium (MTS) and DNA assays, respectively. Human osteoblast-like cells (Saos-2) were placed in contact with epoxy- and amino-functionalized magnetic microparticles ( $1 \times 10^5$  cells ml<sup>-1</sup>). m-PCL and plasma-treated m-PCL microparticles were used as controls to assess the effect of surface functionalization, while Dulbecco's modified Eagle's medium (DMEM) complete medium was used as control for 100 per cent cell viability. Electronic supplementary material, figure S2 and figure 6*a* present MTS and DNA results, respectively. Increasing values of optical density were found with increasing culture time, indicating that none of the tested samples is toxic for Saos-2 cells. The cell viability was found to be above 80 per cent after 7 days of culture when compared with positive control (100%). DNA results showed no detrimental effect on cell proliferation in the presence of the magnetic microparticles (figure 6*a,b*).

### 2.6. CD105+ adipose-derived stem cells isolation from heterogeneous cell suspension: feasibility of the developed immunomagnetic isolation system

One common application of superparamagnetic microparticles is the isolation of stem cell subpopulations,

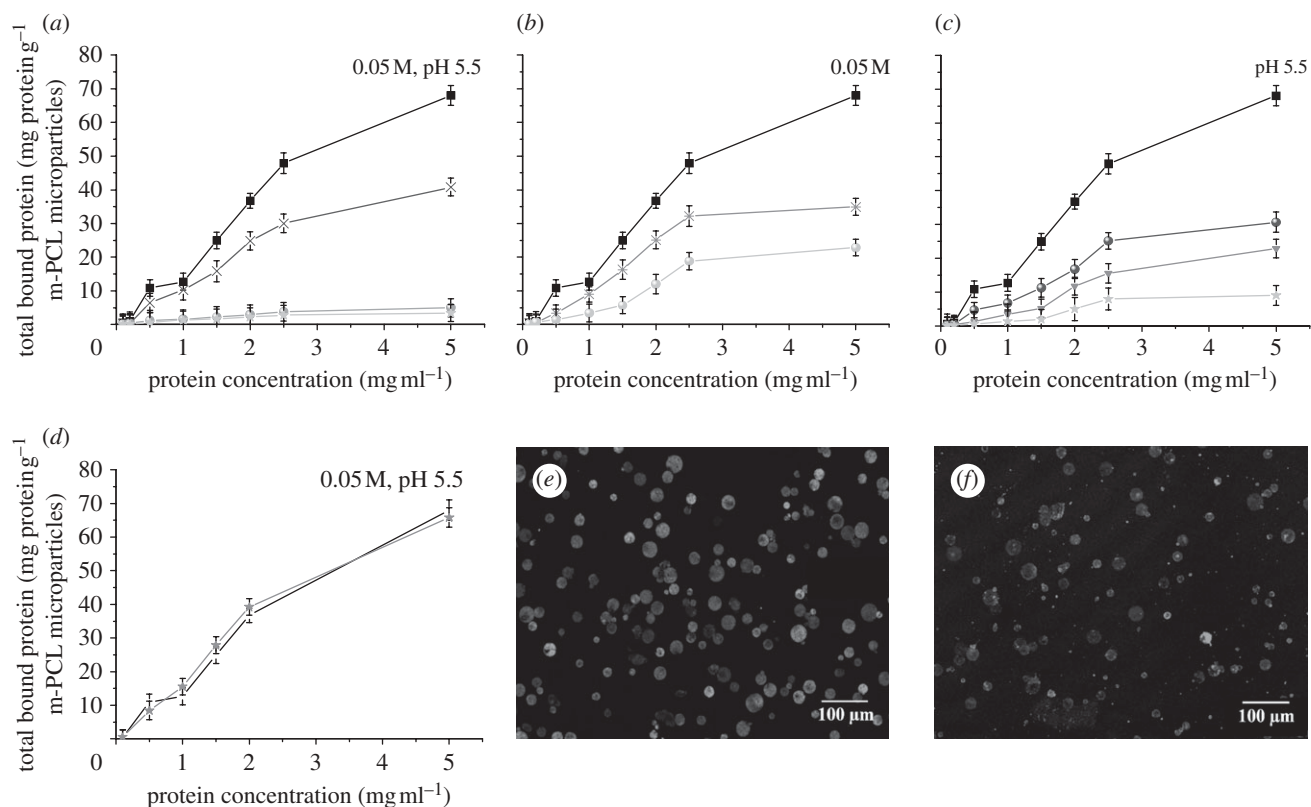


Figure 5. Protein-binding experiments on m-PCL microparticles. Effect of (a) different surface functionalization, (b) pH, (c) ionic strength and (d) incubation time on protein binding. Confocal microscopy images of the (e) amino- and (f) epoxy-functionalized magnetic microparticles after incubation with fluorescein-labelled protein. (a) Filled squares,  $\text{NH}_2$ -m-PCL; crosses, epoxy-m-PCL; grey circles, plasma-m-PCL; stars, m-PCL. (b) Asterisks, pH 3.5; filled squares, pH 5.5; grey circles, pH 7. (c) Filled squares, 0.05 M; filled circles, 0.10 M; grey inverted triangles, 0.50 M; stars, 1.50 M. (d) Incubation time: black line, 5 h; and grey line, overnight.

Table 4. Protein-coupling efficiency on m-PCL microparticles with different surface functionalities (0.05 M MES buffer, pH 5.5, room temperature,  $5 \text{ mg ml}^{-1}$  of initial protein concentration).

sample	bound protein ( $\text{mg g}^{-1}$ ) <sup>a</sup>	protein covalently coupled ( $\text{mg g}^{-1}$ )	coupling yield (%)
m-PCL	$3.42 \pm 2.5$	—	—
plasma-treated m-PCL	$5.00 \pm 2.7$	—	—
epoxy-functionalized m-PCL	$40.79 \pm 2.6$	$19.37 \pm 3.2$	47.49
amino-functionalized m-PCL	$68.04 \pm 3.0$	$48.92 \pm 1.9$	71.90

<sup>a</sup>Total bound protein corresponding to the amount of protein physically bound (adsorbed) plus covalently bound.

namely subpopulations of adipose-derived stem cells (ASCs) [46,47]. Adipose tissue is an abundant source of adult stem cells with multipotent properties suitable for tissue engineering and regenerative medicine [46,48].

Before performing cell isolation experiments with ASCs, we studied the effect of amino-functionalized m-PCL microparticles on their proliferation and morphology. Characteristic morphology of ASCs was observed when they were cultured in contact with the microparticles (figure 6c) as no morphological changes were identified in comparison with controls (cells cultured in the absence of microparticles). After 7 days of culture, the cells were able to adhere to the bottom of the well, spread and proliferate in contact with the magnetic microparticles. The DNA quantification shows good cell proliferation (figure 6b) indicating that the microparticles do not influence the growth and proliferation of the cells.

ASCs have been described as mesenchymal stem cells (MSCs). According to the International Society for Cellular Therapy guidelines, the criteria that define MSCs are adherence to plastic, multipotent differentiation potential and specific surface antigen (Ag) expression (CD105, CD73, CD90) [49]. Antibodies against these molecules will selectively bind to MSCs. Based on that principle, we have coupled CD105 antibody on the surface of the  $\text{NH}_2$ -m-PCL to isolate a specific stem cell population from a mixture of Saos-2 and ASCs. Positive selection of CD105+ cells was successfully performed using the developed superparamagnetic microparticles coupled with CD105 antibody. As shown in figure 6d, the CD105+ population could be isolated with high purity, indicated by the absence of any additional cell population. This result confirms the suitability of the presented system for isolation of CD105+

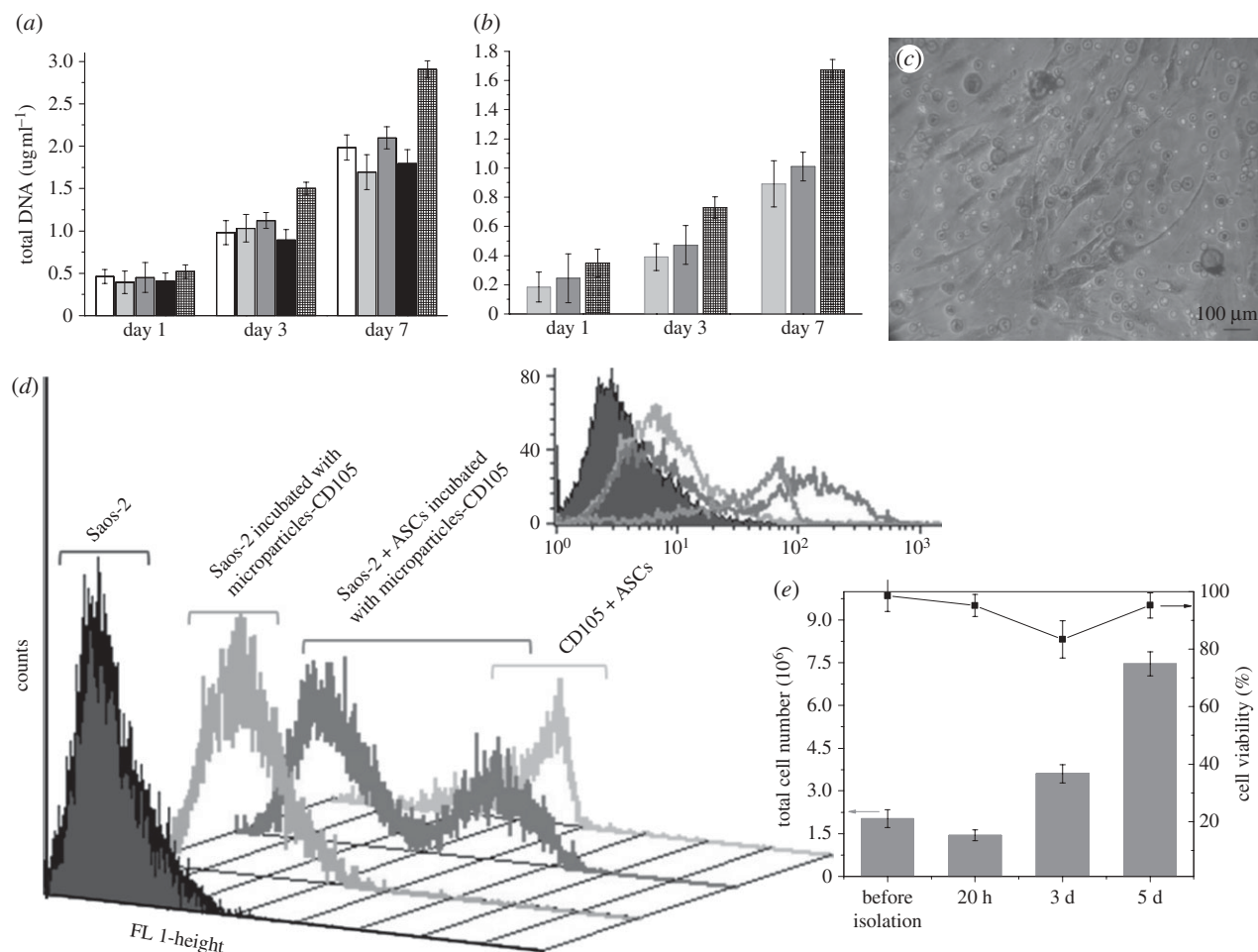


Figure 6. (a) Proliferation of osteoblast-like cells (Saos-2) and (b) ASCs in direct contact with m-PCL microparticles determined by DNA quantification. (c) Optical micrograph of ASCs stained with methylene blue showing the cell morphology after 7 days of culture in contact with the amino-functionalized magnetic microparticles. (d) Flow-cytometry analysis of CD105+ cells (ASCs) isolated from a heterogeneous cell mixture (10 : 1, Saos-2 : ASCs) using amino-functionalized magnetic microparticles previously coupled with anti-CD105 antibody). (e) Viability and total cell number, before and after immunomagnetic isolation procedure, assessed by trypan blue and manual cell count. (a) Unfilled bar, m-PCL; light grey bar, NH<sub>2</sub>-m-PCL; dark grey bar, plasma-m-PCL; black bar, epoxy-m-PCL; checked bar, DMEM 100% control. (b) Light grey bar, NH<sub>2</sub>-m-PCL; dark grey bars, NH<sub>2</sub>-m-PCL-EDC-BSA; checked bar, DMEM control.

cells. In addition, the isolation procedure did not affect the viability of the cells (figure 6e). A slight increase in the number of dead cells was however observed after 3 days of culture. This could be partially mediated by the antibody adhering to the cells. Similar observations have been reported by other authors using different types of immunomagnetic isolation systems [50,51]. Nevertheless, after 5 days of culture, the cells show good viability and morphology. Thus, the system is capable of effectively isolating viable cells for subsequent cultivation and further applications.

### 3. CONCLUSIONS

We have described the synthesis and surface functionalization of magnetite-polymer (Fe<sub>3</sub>O<sub>4</sub>-PCL) microparticles and their utility in cell isolation. m-PCL microparticles could be obtained with spherical shape and different sizes (4–135 μm) by changing the experimental conditions used during their preparation.

A suitable magnetic response was observed by the application of an external magnetic field, allowing the efficient particle separation from a solution, and no significant residual magnetism was measured when removing the field. Amino groups were successfully introduced on the m-PCL microparticles surface by aminolysis, whereas epoxy groups were introduced by plasma grafting. Protein-binding studies on functionalized microparticles showed high coupling yields with low levels of non-specific adsorption, thus suggesting the successful attachment of antibodies to microparticle surfaces and subsequent cell-binding ability.

Additionally, the developed m-PCL microparticles showed excellent biocompatibility in cell-based assays (cell morphology, viability and proliferation) using both Saos-2 and ASCs. CD105-functionalized magnetic particles showed binding specificity to CD105+ cells, thus demonstrating the feasibility of separating CD105+ cells from a heterogeneous cell suspension. We anticipate that the functionalization strategies proposed herein enable a fast and reliable separation

of viable cells and will expand the applications of immuno-magnetic cell-isolation technology.

## 4. EXPERIMENTAL SECTION

### 4.1. Superparamagnetic poly- $\epsilon$ -caprolactone microparticles preparation

PCL superparamagnetic microparticles were prepared by an emulsion-solvent extraction/evaporation method [52], in which synthesized magnetite nanoparticles were entrapped within a polymeric matrix (figure 3a). Briefly, PCL was dissolved in 5 ml of dichloromethane under vigorous stirring. After complete dissolution of the polymer, the magnetite nanoparticles were added. The mixture was sonicated for 10 min at 100 W using an ultrasonic bath (Ultrasons 3001208, J. P. Selecta, Spain) to ensure a good dispersion of the magnetite nanoparticles in the polymeric solution. Subsequently, the suspension was dropped into a continuously stirred PVA solution (100 ml), and emulsified for 4 h at different stirring rates using the dispersing device 'Ultra-Turrax Yellow line DI 18 basic' (IKA, Germany). Different experimental conditions, such as magnetite to polymer ratio, PVA concentration and stirring rate were used (table 1). The m-PCL microparticles were then collected by magnetic separation, washed with distilled water and lyophilized to obtain a fine brownish powder.

### 4.2. Surface functionalization of the superparamagnetic PCL microparticles

**4.2.1. Amino groups: aminolysis of m-PCL microparticles** [39]. Dried m-PCL microparticles were immersed in a 1,6-hexanediamine/2-propanol solution. The microparticles were chemically functionalized at two different temperatures (25 and 37°C) maintaining the reaction vessel under constant agitation (100 r.p.m.) and varying the reaction time from 30 to 90 min. The effect of several reaction conditions on the microparticle functionalization was investigated (table 2). At the end of each treatment period, the amino-functionalized m-PCL (NH<sub>2</sub>-m-PCL) microparticles were collected by magnetic separation and extensively dialysed using deionized distilled water to remove free 1,6-hexanediamine. Finally, NH<sub>2</sub>-m-PCL microparticles were dried in a vacuum desiccator at room temperature until constant weight.

**4.2.2. Epoxide groups: cold plasma and epichlorohydrin reaction.** Epoxide groups were introduced on the surface of the m-PCL microparticles using an adapted methodology, earlier proposed by Larson *et al.* [53] for oxide surfaces of films. The procedure is based on the use of a plasma-activation step followed by chemical reaction. Both plasma activation and chemical functionalization were carried out in a radio-frequency plasma reactor 'PlasmaPrep5' (Gala Instruments, Germany).

Before the experiments, the plasma chamber was thoroughly purged with a continuous flow of the gas (O<sub>2</sub>) used during the treatment to reduce trace amounts of air and moisture. The m-PCL microparticles were

exposed to oxygen plasma. During the treatment, the gas flow (O<sub>2</sub>) was adjusted in order to keep a constant pressure of 0.18 mbar inside the chamber. A power of 90 W was applied. The duration of the surface activation was 2 min. Subsequently, vapours of epichlorohydrin were introduced inside the chamber (vapour pressure 21.1°C at 13.8 mmHg) and allowed to react with the particles for 30 min (electronic supplementary material, scheme S1).

The epoxy-functionalized m-PCL (epoxy-m-PCL) microparticles were then stored under dry controlled conditions, using a vacuum desiccator, to preserve their surface functionality.

### 4.3. Protein-binding experiments

BSA was selected as a model protein to study the ability of the functionalized m-PCL microparticles to bind protein molecules. For NH<sub>2</sub>-m-PCL microparticles, a typical carbodiimide (EDC) activation-coupling experiment was carried out [42]. Briefly, 10 mg of dried NH<sub>2</sub>-m-PCL microparticles were resuspended in 0.05 M MES buffer followed by the addition of a freshly prepared EDC solution (40 mg ml<sup>-1</sup> in 0.05 M MES). The suspension was carefully mixed for 15 min at room temperature. Subsequently, BSA, dissolved in MES buffer, was added. The suspension was mixed on an orbital shaker for two different time periods (5 h and overnight) and at two different temperatures (25°C and 37°C). The microparticles were washed, resuspended in MES buffer and stored at 4°C for further analysis. To quantify the coupling efficiency, the protein-bound microparticles were immersed in buffer medium containing 1 per cent Tween 20, which removes only the physically bound (adsorbed) protein [54,55]. After elution, the supernatant was analysed for protein quantification. The protein concentration in the supernatants was determined by absorbance measurement at 280 nm in a UV-vis spectrophotometer. The amount of covalently bound protein was determined by the difference in initial protein concentration and the concentration of protein remaining in the supernatants.

When epoxy-m-PCL microparticles were used, the particles were washed in MES buffer and subsequently mixed with protein solution. The experimental procedure was identical to that previously described for NH<sub>2</sub>-m-PCL microparticles.

The effect of several experimental parameters on the covalent binding of BSA to the surface-functionalized microparticles was studied. The pH was varied in the range of 3.5–7 (MES buffer, 0.05 M). The influence of the ionic strength was investigated by adding different concentrations of NaCl (0.1, 0.5 and 1.5 M) to the buffer solution.

### 4.4. Isolation of a specific subpopulation of human adipose-derived stem cells

**4.4.1. Coupling of mouse anti-human CD105-FITC monoclonal antibody to the NH<sub>2</sub>-m-PCL microparticles.** The preparation of the superparamagnetic systems for cell isolation includes the coupling of specific ligand to bind to the receptors present in the surface of the

target cell. The available primary amino groups on NH<sub>2</sub>-m-PCL microparticles allow for the coupling of protein-like molecules through their carboxylic acid groups following, for instance, carbodiimide activation. The experimental procedure followed in this case was identical to that previously described for BSA coupling, but using CD105 (mouse anti-human CD105 monoclonal antibody (endoglin) conjugated with FITC; AbD Serotec, UK) as ligand. In brief, approximately  $1 \times 10^6$  dried NH<sub>2</sub>-m-PCL microparticles were resuspended in 0.05 M MES buffer for 1–2 min allowing the hydration of the particles. Subsequently, the tubes were placed near a magnet for 4 min and the supernatant was removed. This washing procedure was repeated for at least three times, followed by the addition of a freshly prepared EDC solution in 0.05 M MES buffer. Subsequently, 1 µg of CD105-FITC was added to the particle suspension in MES buffer. The system was protected from the light and placed in an orbital shaker overnight at room temperature. The tubes containing the NH<sub>2</sub>-m-PCL microparticles coupled with CD105-FITC were then placed near a magnet and the supernatant was carefully removed. The washing procedure was repeated maintaining the anti-CD105-coupled microparticles stored in PBS solution (0.01 M, pH 7.4) at 4°C for further cell-isolation procedure.

**4.4.2. Cell isolation.** The ability of the functionalized m-PCL microparticles to isolate specific cell subpopulations from a heterogeneous cell mixture was tested using a cell suspension of osteoblast-like cells (Saos-2) and human-derived ASCs. For that, both cell types were individually cultured until confluence in DMEM (Sigma-Aldrich, USA) supplemented with 10 per cent of heat-inactivated foetal bovine serum (FBS, Biochrom AG, Germany) and 1 per cent of antibiotic/antimycotic solution (Sigma-Aldrich), from now on referred to as DMEM complete medium, in humidified atmosphere with 5 per cent CO<sub>2</sub> at 37°C. The culture medium was replenished every 2 days. Cells at the same passages (2, 3, 5) and identical culture times were individually harvested and mixed together to obtain 1 ml of heterogeneous cell suspension (10:1, Saos-2:ASCs) in PBS. About  $1 \times 10^6$  CD105-FITC-coupled microparticles were used for  $2 \times 10^5$  target ASCs in the heterogeneous suspension. The suspension containing both cell types was incubated with the magnetic microparticles coupled with the fluorescent CD105 antibody. The mixture was incubated in an orbital shaker for 20 min at 4°C in light-protected tubes. The tubes were then placed near a magnet for 2 min and the supernatant containing the unbound cells removed. The positive cells bound to CD105-FITC-coupled magnetic microparticles were washed at least three times. The samples were finally resuspended in acquisition buffer for further flow-cytometric analysis.

This work was supported through the European Union-funded projects: Marie Curie Host Fellowships for Early Stage Research Training (EST) 'Alea Jacta EST' (MEST-CT-2004-008104), which provided E. R. Balmayor with a PhD Fellowship, and Network of Excellence EXPERTISSUES

(NMP3-CT-2004-500283). A. M. Frias thanks the Portuguese Foundation for Science Technology for a post-doctoral fellowship (SFRH/BPD/45206/2008). The authors are grateful to Prof. Bernardo G. Almeida from the Physics Department at University of Minho for his assistance with vibrational magnetometry studies.

## REFERENCES

- Horak, D., Babic, M., Mackova, H. & Benes, M. J. 2007 Preparation and properties of magnetic nano- and micro-sized particles for biological and environmental separations. *J. Sep. Sci.* **30**, 1751–1772. (doi:10.1002/jssc.200700088)
- Safarik, I. & Safarikova, M. 1999 Use of magnetic techniques for the isolation of cells. *J. Chromatogr. B: Biomed. Appl.* **722**, 33–53. (doi:10.1016/S0378-4347(98)00338-7)
- Gupta, A. K. & Gupta, M. 2005 Synthesis and surface engineering of iron oxide nanoparticles for biomedical applications. *Biomaterials* **26**, 3995–4021. (doi:10.1016/j.biomaterials.2004.10.012)
- Franzreb, M., Siemann-Herzberg, M., Hobley, T. J. & Thomas, O. R. T. 2006 Protein purification using magnetic adsorbent particles. *Appl. Microbiol. Biotechnol.* **70**, 505–516. (doi:10.1007/s00253-006-0344-3)
- Gu, H. W., Xu, K. M., Xu, C. J. & Xu, B. 2006 Biofunctional magnetic nanoparticles for protein separation and pathogen detection. *Chem. Commun.* **9**, 941–949. (doi:10.1039/b514130c)
- Safarik, I. & Safarikova, M. 2004 Magnetic techniques for the isolation and purification of proteins and peptides. *BioMagn. Res. Technol.* **2**, 7–24. (doi:10.1186/1477-044X-2-7)
- Häfeli, U. O. 2004 Magnetically modulated therapeutic systems. *Int. J. Pharm.* **277**, 19–24. (doi:10.1016/j.ijpharm.2003.03.002)
- Mornet, S., Vasseur, S., Grasset, F. & Duguet, E. 2004 Magnetic nanoparticle design for medical diagnosis and therapy. *J. Mater. Chem.* **14**, 2161–2175. (doi:10.1039/b402025a)
- Schillinger, U., Brill, T., Rudolph, C., Huth, S., Gersting, S., Krotz, F., Hirschberger, J., Bergemann, C. & Plank, C. 2005 Advances in magnetofection: magnetically guided nucleic acid delivery. *J. Magn. Magn. Mater.* **293**, 501–508. (doi:10.1016/j.jmmm.2005.01.032)
- Neuberger, T., Schopf, B., Hofmann, H., Hofmann, M. & von Rechenberg, B. 2005 Superparamagnetic nanoparticles for biomedical applications: possibilities and limitations of a new drug delivery system. *J. Magn. Magn. Mater.* **293**, 483–496. (doi:10.1016/j.jmmm.2005.01.064)
- Hamoudeh, M. & Fessi, H. 2006 Preparation, characterization and surface study of poly-epsilon caprolactone magnetic microparticles. *J. Colloid Interface Sci.* **300**, 584–590. (doi:10.1016/j.jcis.2006.04.024)
- Landfester, K. & Ramirez, L. P. 2003 Encapsulated magnetite particles for biomedical application. *J. Phys.: Condens. Matter* **15**, S1345–S1361. (doi:10.1088/0953-8984/15/15/304)
- Ramirez, L. P. & Landfester, K. 2003 Magnetic polystyrene nanoparticles with a high magnetite content obtained by miniemulsion processes. *Macromol. Chem. Phys.* **204**, 22–31. (doi:10.1002/macp.200290052)
- Kim, D. H., Lee, S. H., Im, K. H., Kim, K. N., Kim, K. M., Shim, I. B., Lee, M. H. & Lee, K. 2006 Surface-modified magnetite nanoparticles for hyperthermia: preparation, characterization, and cytotoxicity studies.

- Curr. Appl. Phys.* **6**, e242–e246. (doi:10.1016/j.cap.2006.01.048)
- 15 Yang, J., Park, S. B., Yoon, H. G., Huh, Y. M. & Haam, S. 2006 Preparation of poly epsilon-caprolactone nanoparticles containing magnetite for magnetic drug carrier. *Int. J. Pharm.* **324**, 185–190. (doi:10.1016/j.ijpharm.2006.06.029)
  - 16 Bayramoglu, G., Logoglu, E. & Arica, M. Y. 2007 Cytochrome *c* adsorption on glutamic acid ligand immobilized magnetic poly(methylmethacrylate-co-glycidylmethacrylate) beads. *Coll. Surf. A: Physicochem. Eng. Aspects* **297**, 55–62. (doi:10.1016/j.colsurfa.2006.10.023)
  - 17 Caruso, F., Spasova, M., Susha, A., Giersig, M. & Caruso, R. L. 2001 Magnetic nanocomposite particles and hollow spheres constructed by a sequential layering approach. *Chem. Mater.* **13**, 109–116. (doi:10.1021/cm001164h)
  - 18 de Santa Maria, L. C., Leite, M. C. A. M., Costa, M. A. S., Ribeiro, J. M. S., Senna, L. F. & Silva, M. R. 2004 Characterization of magnetic microspheres based on network styrene and divinylbenzene copolymers. *Mater. Lett.* **58**, 3001–3006. (doi:10.1016/j.matlet.2004.05.028)
  - 19 Benoit, M. A., Baras, B. & Gillard, J. 1999 Preparation and characterization of protein-loaded poly(caprolactone) microparticles for oral vaccine delivery. *Int. J. Pharm.* **184**, 73–84. (doi:10.1016/S0378-5173(99)00109-X)
  - 20 Chen, D. R., Bei, J. Z. & Wang, S. G. 2000 Polycaprolactone microparticles and their biodegradation. *Polym. Degrad. Stab.* **67**, 455–459. (doi:10.1016/S0141-3910(99)00145-7)
  - 21 Luong-Van, E., Grøndahl, L., Chua, K. N., Leong, K. W., Nurcombe, V. & Cool, S. M. 2006 Controlled release of heparin from poly(caprolactone) electrospun fibers. *Biomaterials* **27**, 2042–2050. (doi:10.1016/j.biomaterials.2005.10.028)
  - 22 Pitt, C. G. 1990 Poly(caprolactone) and its co-polymers. In *Biodegradable polymers as drug delivery systems* (eds M. Chasin & R. Langer), pp. 71–120. New York, NY: Marcel Dekker.
  - 23 Nair, L. S. & Laurencin, C. T. 2007 Biodegradable polymers as biomaterials. *Progr. Polymer Sci.* **32**, 762–798. (doi:10.1016/j.progpolymsci.2007.05.017)
  - 24 Carrot, G., Hilborn, J. G., Trollss, M. & Hedrick, J. L. 1999 Two general methods for the synthesis of thiol-functional polycaprolactones. *Macromolecules* **32**, 5264–5269. (doi:10.1021/ma990198b)
  - 25 Santiago, L. Y., Nowak, R. W., Rubin, J. P. & Marra, K. G. 2006 Peptide-surface modification of poly(caprolactone) with laminin-derived sequences for adipose-derived stem cell applications. *Biomaterials* **27**, 2962–2969. (doi:10.1016/j.biomaterials.2006.01.011)
  - 26 Cortez, C., Tomaskovic-Crook, E., Johnston, A. P. R., Scott, A. M., Nice, E. C., Heath, J. K. & Caruso, F. 2007 Influence of size, surface, cell line, and kinetic properties on the specific binding of A33 antigen-targeted multilayered particles and capsules to colorectal cancer cells. *ACS Nano* **1**, 93–102. (doi:10.1021/nn700060m)
  - 27 Basinska, T. 2005 Hydrophilic core-shell microspheres: a suitable support for controlled attachment of proteins and biomedical diagnostics. *Macromol. Biosci.* **5**, 1145–1168. (doi:10.1002/mabi.200500138)
  - 28 Sarobe, J., Molina-Bolivar, J. A., Forcada, J., Galisteo, F. & Hidalgo-Álvarez, R. 1998 Functionalized monodisperse particles with chloromethyl groups for the covalent coupling of proteins. *Macromolecules* **31**, 4282–4287. (doi:10.1021/ma9707143)
  - 29 Olsvik, O., Popovic, T., Skjerve, E., Cudjoe, K. S., Hornes, E., Ugelstad, J. & Uhlen, M. 1994 Magnetic separation techniques in diagnostic microbiology. *Clin. Microbiol. Rev.* **7**, 43–54.
  - 30 Khalafalla, S. E. & Reimers, G. W. 1974. *Production of magnetic fluids by peptization techniques*. US patent no. 3843540. See <http://www.freepatentonline.com/3843540.pdf>.
  - 31 DynalBiotech. 2008 The principle of dynabeads. See [http://www.invitrogen.com/site/us/en/home/brands/Dynal/dynabeads\\_technology.html](http://www.invitrogen.com/site/us/en/home/brands/Dynal/dynabeads_technology.html).
  - 32 Pamme, N. & Wilhelm, C. 2006 Continuous sorting of magnetic cells via on-chip free-flow magnetophoresis. *Lab Chip* **6**, 974–980. (doi:10.1039/b604542a)
  - 33 Balmayor, E. R., Tuzlakoglu, K., Azevedo, H. S. & Reis, R. L. 2009 Preparation and characterization of starch-poly-ε-caprolactone microparticles incorporating bioactive agents for drug delivery and tissue engineering applications. *Acta Biomater.* **5**, 1035–1045. (doi:10.1016/j.actbio.2008.11.006)
  - 34 Mohamed, A., Gordon, S. H. & Biresaw, G. 2007 Polycaprolactone/polystyrene bioblends characterized by thermogravimetry, modulated differential scanning calorimetry and infrared photoacoustic spectroscopy. *Polym. Degrad. Stab.* **92**, 1177–1185. (doi:10.1016/j.polymdegradstab.2007.04.012)
  - 35 Yang, T. I., Brown, R. N. C., Kempel, L. C. & Kofinas, P. 2008 Magneto-dielectric properties of polymer-Fe<sub>3</sub>O<sub>4</sub> nanocomposites. *J. Magn. Magn. Mater.* **320**, 2714–2720. (doi:10.1016/j.jmmm.2008.06.008)
  - 36 Park, T.-J. & Wong, S. S. 2006 As-prepared single-crystalline hematite rhombohedra and subsequent conversion into monodisperse aggregates of magnetic nanocomposites of iron and magnetite. *Chem. Mater.* **18**, 5289–5295. (doi:10.1021/cm061503s)
  - 37 Redl, F. X., Black, C. T., Papaefthymiou, G. C., Sandstrom, R. L., Yin, M., Zeng, H., Murray, C. B. & O'Brien, S. 2004 Magnetic, electronic, and structural characterization of nonstoichiometric iron oxides at the nanoscale. *J. Am. Chem. Soc.* **126**, 14583–14599. (doi:10.1021/ja046808r)
  - 38 Shi, Y. 2006 Superparamagnetic nanoparticles for magnetic resonance imaging (MRI) diagnosis. Master of Engineering Science thesis, The University of Adelaide, SA, Australia.
  - 39 Zhu, Y. B., Gao, C. Y., Liu, X. Y. & Shen, J. C. 2002 Surface modification of polycaprolactone membrane via aminolysis and biomacromolecule immobilization for promoting cytocompatibility of human endothelial cells. *Biomacromolecules* **3**, 1312–1319. (doi:10.1021/bm020074y)
  - 40 Li, Y., Lee, J., Lal, J., An, L. & Huang, Q. 2008 Effects of pH on the interactions and conformation of bovine serum albumin: comparison between chemical force microscopy and small-angle neutron scattering. *J. Phys. Chem. B* **112**, 3797–3806. (doi:10.1021/jp077392h)
  - 41 Peng, Z. G., Hidajat, K. & Uddin, M. S. 2004 Conformational change of adsorbed and desorbed bovine serum albumin on nano-sized magnetic particles. *Colloids Surf. B: Biointerfaces* **33**, 15–21. (doi:10.1016/j.colsurfb.2003.08.007)
  - 42 Hermanson, G. 1996 Functional targets. In *Bioconjugate techniques* (ed. G. Hermanson), 1st edn, pp. 114–116. San Diego, CA: Academic Press, Inc.
  - 43 Su, Y. L. & Li, C. 2008 Controlled adsorption of bovine serum albumin on poly(acrylonitrile)-based zwitterionic membranes. *React. Funct. Polym.* **68**, 161–168. (doi:10.1016/j.reactfunctpolym.2007.10.001)
  - 44 Andrade, J. D. 1985 Protein adsorption. In *Surface and interfacial aspects of biomedical polymers* (ed. J. D. Andrade), pp. 1–80. New York: Plenum Press.
  - 45 Ortega-Vinuesa, J. & Hidalgo-Álvarez, R. 1995 Sequential adsorption of F(ab)<sub>2</sub> and BSA on negatively and positively charged polystyrene latexes. *Biotechnol. Bioeng.* **47**, 633–639. (doi:10.1002/bit.260470604)

- 46 Park, B. H., Jung, J. C., Lee, G. H., Kim, T. J., Lee, Y. J., Kim, J. Y., Kim, Y. W., Jeong, J. H. & Chang, Y. M. 2008 Comparison of labeling efficiency of different magnetic nanoparticles into stem cell. *Coll. Surf. A: Physicochem. Eng. Aspects* **313**, 145–149. (doi:10.1016/j.colsurfa.2007.04.152)
- 47 Rada, T., Reis, R. L. & Gomes, M. E. 2009 Novel method for the isolation of adipose stem cells (ASCs). *J. Tissue Eng. Regen. Med.* **3**, 158–159. (doi:10.1002/term.141)
- 48 Rodriguez, A. M., Elabd, C., Amri, E. Z., Ailhaud, G. & Dani, C. 2005 The human adipose tissue is a source of multipotent stem cells. *Biochimie* **87**, 125–128. (doi:10.1016/j.biochi.2004.11.007)
- 49 Dominici, M. *et al.* 2006 Minimal criteria for defining multipotent mesenchymal stromal cells. The International Society for Cellular Therapy position statement. *Cytotherapy* **8**, 315–317. (doi:10.1080/14653240600855905)
- 50 Konishi, Y., Lindholm, K., Yang, L.-B., Li, R. & Shen, Y. 2002 Isolation of living neurons from human elderly brains using the immunomagnetic sorting DNA-linker system. *Am. J. Pathol.* **161**, 1567–1576.
- 51 Tokairin, T., Nishikawa, Y., Doi, Y., Watanabe, H., Yoshioka, T., Su, M., Omori, Y. & Enomoto, K. 2002 A highly specific isolation of rat sinusoidal endothelial cells by the immunomagnetic bead method using SE-1 monoclonal antibody. *J. Hepatol.* **36**, 725–733. (doi:10.1016/S0168-8278(02)00048-X)
- 52 Lewis, D. H. 1990 Controlled release of bioactive agents from lactide/glycolide polymers. In *Biodegradable polymers as drug delivery systems* (eds M. Chasin & R. Langer), pp. 1–42. New York, NY: Marcel Dekker, Inc.
- 53 Larson, B. J., Helgren, J. M., Manolache, S. O., Lau, A. Y., Lagally, M. G. & Denes, F. S. 2005 Cold-plasma modification of oxide surfaces for covalent biomolecule attachment. *Biosens. Bioelectron.* **21**, 796–801. (doi:10.1016/j.bios.2005.02.005)
- 54 Peula, J. M., Hidalgo-Alvarez, R. & Nieves, F. J. D. 1998 Covalent binding of proteins to acetal-functionalized latexes. I. Physics and chemical adsorption and electrokinetic characterization. *J. Coll. Interface Sci.* **201**, 132–138. (doi:10.1006/jcis.1997.5388)
- 55 Ortega-Vinuesa, J. L., Bastos-González, D. & Hidalgo-Alvarez, R. 1995 Comparative studies on physically adsorbed and chemically bound IgG to carboxylated latexes, II. *J. Colloid Interface Sci.* **176**, 240–247. (doi:10.1006/jcis.1995.0027)